

# Uniform and Concentric Circular Antenna Arrays Synthesis for Smart Antenna Systems Using Artificial Neural Network Algorithm

Bilel Hamdi\*, Selma Limam, and Taoufik Aguli

**Abstract**—Recently, researchers were interested in neural algorithms for optimization problems for several communication systems. This paper shows a novel algorithm based on neural technique presented to enhance the performance analysis of beam-forming in smart antenna technology using  $N$  elements for Uniform Circular Array (UCA) and Concentric Circular Array (CCA) geometries. To demonstrate the effectiveness and reliability of the proposed approach, simulation results are carried out in MATLAB. The radiators are considered isotropic, and hence mutual coupling effects are ignored. The proposed array shows a considerable improvement against the existing structures in terms of 3-D scanning, size, directivity, HPBW and SLL reduction. The results show that multilayer feed-forward neural networks are robust and can solve complex antenna problems. However, artificial neural network (ANN) is able to generate very fast the results of synthesis by using generalization with early stopping method. Important gain in the running time and memory used is obtained using this latter method for improving generalization (called early stopping). To validate this work, several examples are shown.

## 1. INTRODUCTION

Adaptive beam-forming capabilities for smart antenna arrays are nowadays used to improve the performance of mobile and wireless communication systems. Due to the current interest of the known circular antenna arrays that have several advantages over other types of array antenna configurations, it is becoming increasingly important in the electromagnetic designs of future electronic applications such as: sonar, radar, mobile, commercial satellite communications systems, beam forming network, and a receiver or transmitter [2, 3].

Considering the diversity of aims searched by users, the increase in performance requirements for antenna arrays makes it necessary to extend current array synthesis methodologies to circular ring array, creating a new research problem (e.g., conformal phased array antenna). The latest circular geometry, also known as concentric circular array (CCA), is a planar array that contains many concentric circular rings of different radii and number of element. Its benefits including the flexibility in array pattern synthesis and design both in narrowband and broadband beam-forming applications especially at the base stations (in mobile radio communications system) [2]. However, uniformly excited and equally spaced circular ring array offers high directivity but suffers from high side lobe level (SLL) [1, 5].

Generally, antenna synthesis was started to require on intelligent systems such that genetic algorithms and neural network. Several articles shows that genetic algorithm (GA) is mainly used for side lobe reduction in the array pattern synthesis [6]. But, artificial neural network (ANN) have been studied in various application like pattern recognition systems, and have been exploited for input-output mapping, for system identification, for adaptive prediction, etc.... Therefore, we are interested to present in this paper the neural networks method that will be applied to the array pattern synthesis, highlighting their most important features and distinctive characters [8, 9].

---

*Received 15 March 2016, Accepted 23 April 2016, Scheduled 5 May 2016*

\* Corresponding author: Bilel Hamdi (hamdibilel1985@gmail.com).

The authors are with the Laboratory of the Communication Systems Sys'Com (LR-99-ES21), National Engineering School of Tunis, University of Tunis El Manar, BP. 37 Le Belvédère, Tunis 1002, Tunisia.

In the interest of the best approximation property, this approach permits to model and optimize the antenna arrays system, by acting on many parameters of the array and taking into account predetermined general criteria. The goal is then to build a feedforward neural network with supervised learning that approximates the following array pattern's function [14–16].

This study can show some fundamental details about the optimal size of a feedforward Neural Network to avoid over-fitting problems. After that sub-data sets will be created for training, test and validation, and then feed-forward neural network will be created and trained [18]. The output values will be generated and denormalized, and finally the performance of the neural network will be checked by comparing the output values with target values [12, 13].

This fact increases the complexity of the problem under consideration and fitting the neural network model, such as training function, architecture and parameter, that would improve and result more accuracy about input-output relations [10, 11].

Our main aim here is to consider the antenna array synthesis for regular uniform circular antenna Arrays geometries and especially in the extended concentric circular antenna Arrays [4, 5].

For the reason that the adoption of the neural network training algorithm as numerical optimization techniques, a few popular architectures are described to illustrate the need to develop an specific architecture to another problem. Several cases that still need to be addressed for solving practical problems using artificial neural network (ANN) approach are given [9, 15, 17].

This paper is organized as follows: in Section 2 the theoretical background of the array factor analysis including pattern synthesis is reminded, in particular uniform concentric circular antenna arrays. The basics of artificial neural networks (ANN) and their applications are recalled in Section 3. It explains how to introduce the basic principles of artificial neural network (ANN), some fundamental networks are examined in detail for their ability to solve simple pattern synthesis problem. These fundamental networks together with the principles of artificial neural network (ANN) will lead to the development of architectures for complex (3D) periodic array antennas synthesis (conformal cylindrical phased Arrays). The following section illustrates the numerical results and discussions. In the final section, some conclusions are drawn.

## 2. PROBLEM FORMULATION: CONCENTRIC RINGS ARRAY MODEL

This paper addresses efficient beamforming techniques for concentric circular antenna arrays (CCAA) [10]. The proposed geometry of a concentric circular antenna array is shown in Figure 1. Where there are  $M$  concentric circular rings and the  $m$ th ring has a radius  $r_m$  and the corresponding number of elements is  $N_m$  where  $m = 1; 2; \dots; M$ . Assuming that all elements are isotropic sources (in all the rings), then the array factor of the considered configuration on the  $x$ - $y$  plane with central element feeding (Figure 1) may be written as the following relation [1, 4, 5]:

$$AF = 1 + \sum_{m=1}^M \sum_{i=1}^{N_m} W_m e^{j(K r_m \sin(\theta) \cos(\phi - \phi_{mi}) + \alpha_{mi})} \quad (1)$$

with:

$M$  = number of rings;

$N_m$  = number of elements in ring  $m$ ;

$W_m$  = excitation current of elements on  $m$ th ring;

$r_m$  = radius of ring  $m = \frac{N_m d_m}{2\pi}$ ;

$d_m$  = interelement spacing of  $m$ th ring;

$k$  = wave number =  $\frac{2\pi}{\lambda}$ ;

$\lambda$  = signal wavelength;

$j$  = complex number;

$\theta$  = the zenith angle from the positive  $z$  axis;

$\phi$  = the azimuth angle from the positive  $x$  axis;

$\phi_{mi}$  = element angular separation measured from the positive  $x$  axis given by:

$$\phi_{mi} = 2\pi \left( \frac{(i-1)}{2\pi} \right); \quad m = 1; \dots; M; \quad i = 1; \dots; N_m \quad (2)$$

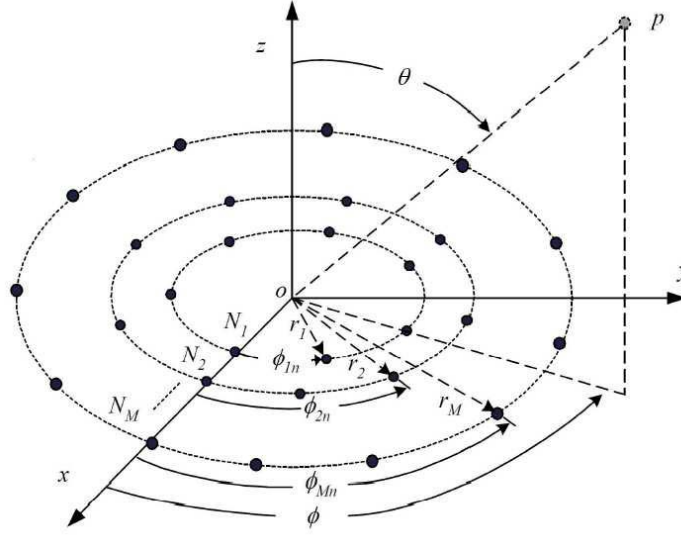


**Figure 1.** Geometry of concentric circular antenna array.

$\alpha_{mi}$  the phase difference between the individual elements in the array given by:

$$\alpha_{mi} = kr_m \sin(\theta_0) \cos(\phi_0 - \phi_{mi}); \quad m = 1; \dots; M; \quad i = 1; \dots; N_m \quad (3)$$

where  $\theta_0$  and  $\phi_0$  are the values of  $\theta$  and  $\phi$  ( $\theta, \phi \in [-\pi; \pi]$ ) respectively where the maximum peak of main lobe is given. If  $\theta_0 =$  and  $\phi =$  constant, the radiation pattern will be a broadside array pattern. Next, The array factor in this case is given below:

$$AF = 1 + \sum_{m=1}^M \sum_{i=1}^{N_m} W_m e^{j(Kr_m \sin(\theta) \cos(\phi - \phi_{mi}))} \quad (4)$$

This latter relation leads to indicate that the normalized absolute array factor in dB can be expressed as:

$$AF \text{ (dB)} = 20 \times \log_{10} \left( \frac{|AF|}{|AF|_{\max}} \right) \quad (5)$$

The notation of  $u, v$  indicates the unit direction:

$$\begin{aligned} u &= \sin(\theta) \sin(\phi) - \sin(\theta_0) \sin(\phi_0) \\ v &= \sin(\theta) \cos(\phi) - \sin(\theta_0) \cos(\phi_0) \end{aligned} \quad (6)$$

The pair  $(\theta_0, \phi_0)$  is taken as the steering direction and the pair  $(\theta, \phi)$  indicates the arrival direction. In this work, two kinds of  $u$ - $v$  space were assumed for SLL reduction: one is regular  $u$ - $v$  space where the steering direction  $(\theta_0, \phi_0) = (0, 0)$ , and  $u, v \in [-1, 1]$ . The other is extended  $u$ - $v$  space where the steering direction  $(\theta_0, \phi_0) \neq (0, 0)$ . Consequently, the value of  $u$  and  $v$  varies against the steering direction and belongs to  $[-2, 2]$  for any combination of the arrival and steering directions. Provided that the  $u$ - $v$  space allows one to synthesize an array structure that verifies a beam pattern with desired profile for whatever steering direction [5, 7].

### 3. ARTIFICIAL NEURAL NETWORKS (ANN) PRINCIPLES

In this section, it is important to explain clearly the artificial neural network (ANN) as a powerful computational model that has been successfully used to simulate the features and behaviors of the antenna arrays [9, 16, 17].

The benefit of neural networks includes many areas of research that involves building a model of the brain and training the latter model to recognize certain types of patterns especially for the synthesis and optimization of antenna arrays [14, 15].

### 3.1. Model of an Artificial Neural Network

The above Figure 3 represents the simple model of an artificial neuron system that can be inspired by biological nervous systems, such as the brain, process information (see Figure 2) [12, 13]. It is composed of a large number of highly interconnected processing elements (neurons) working in unison to solve specific problems. Every component of the structure bears a direct analogy to the actual constituents of a biological neuron and hence it is termed as artificial neuron [9]. In this model which explains and performs the basis function of artificial neural networks. Here, we consider  $x_1, x_2, \dots, x_n$  are the  $n$  inputs to the artificial neuron and  $w_1, w_2, \dots, w_n$  are the weights associated to the input links.

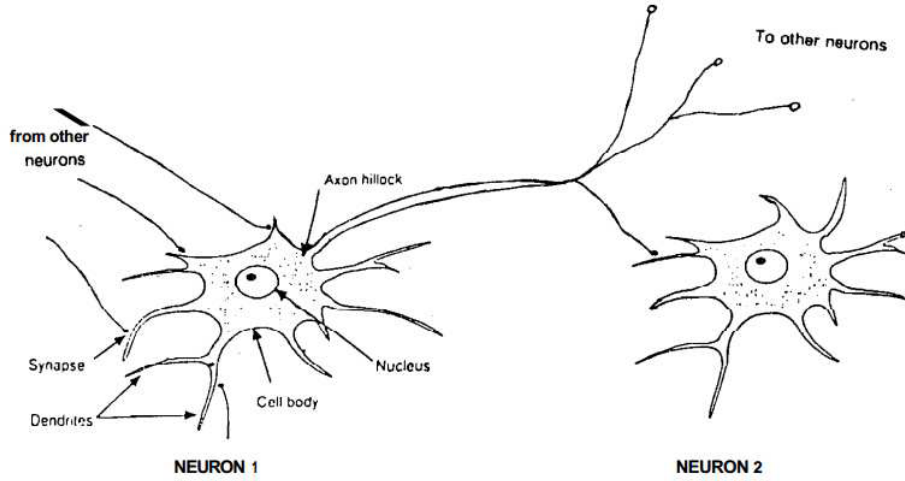


**Figure 2.** Biological neuron.

Next, a feedforward neural network that is also known as Multi-Layer Perceptrons (MLP) is established with a classification algorithm deduced by the neuronal response. The biological neuron receives all inputs through the dendrites, sums them and produces an output, if the sum is greater than a threshold value. The input signals are passed on to the cell body. So, the data inputs pass through the network, layer by layer, until it is received by the soma of the artificial neuron at the outputs:

$$I = w_1x_1 + w_2x_2 + \dots + w_nx_n = \sum_{i=1}^n w_ix_i \quad (7)$$

To result the final output  $y$ , the sum is passed on to a nonlinear filter known as an activation function which releases the output  $y$ .

$$y = f(I) \quad (8)$$

where  $f$  can be a simple threshold function or a sigmoidal, hyperbolic tangent or radial basis function.

In this work, we used the Levenberg-Marquardt feedforward backpropagation algorithm to train and simulate the network. Neural networks with backpropagation algorithm were used to derive the models for time-varying positioning error tracking. It is a supervised learning example by which a layered feedforward network with continuously valued processing elements is trained for nonlinear pattern mapping. The difference between the target value and network output propagates backward during training to adjust the weights so that the network can occur the matching output pattern when the corresponding input pattern values are given. Feedforward backpropagation network uses feedforward neuron connections and is trained with supervised backpropagation learning rule. Network is trained by providing it with input data (phases, amplitudes, distance... etc.) and the corresponding output data (8). The objective of training is to modify the biases and weights of the network to minimize the error function and to finish with desired output for all possible values of input feed. After deciding the neural network architecture (see Figure 4) with definite structure the network is ready to be trained [12, 13]. Previously, three kinds of data sets (inputs) are used, namely the training set, the validation set and the test set. The training set is a set of values which contain information

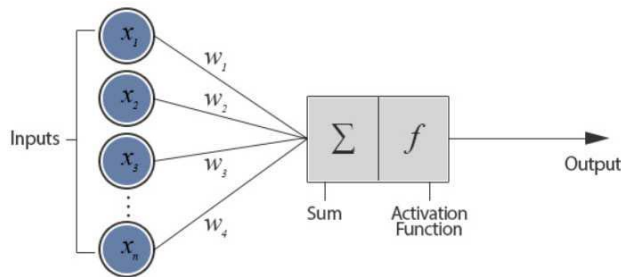


**Figure 3.** Simple model of an artificial neuron.

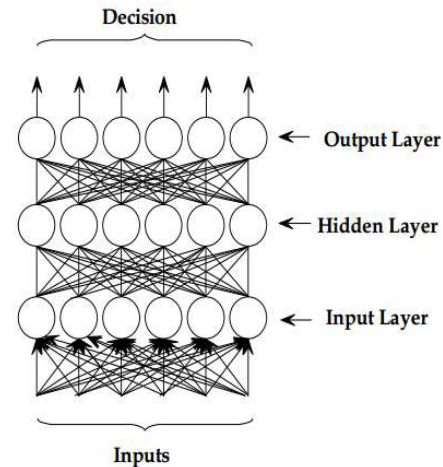


**Figure 4.** Neural network architecture (Multi-Layer Back propagation NN).

about the target function for training the network. The validation set is associated with the early stopping technique. During the training phase, the validation error is monitored in order to prevent the network from over-fitting the training data. Normally, the test set is just used to evaluate the network performance afterwards. 60% of the data is used for training the network and remaining 40% is equally used respectively for validating and testing the network to unlearned inputs [18]. Precisely, the application randomly divides input vectors and target vectors into three known sets as follows:

- 60% are used for training.
- 20% are used to validate that the network is generalizing and to stop training before overfitting.
- The last 20% are used as a completely independent test of network generalization.

### 3.2. Methodology

The Neural Network has to be trained with the given sets of input-output data. The radiation pattern is exploited as the input data and the design parameters are used as the output data. The array factor can be sampled at different angles and given to the neural network. But, to describe the pattern correctly, so, a large number of samples are needed. Moreover, the number varies with the complexity of the pattern problem. A large sample leads to a large number of input nodes for the neural network. A large neural network is hard to implement and requires a lot of data and time for training [8, 9, 15]. In order to reduce the number of nodes and to learn the desired magnitude of the array factor at the same time avoid overfitting, validation or early stopping is often used. To minimize the risk of overfitting, one is tempted to use the smallest network possible. A regularization term may be added in the training criterion to explicitly penalize the network complexity, which is also equivalent to adding noise in training data [18].

A significant connection between Neural Network and array antenna is established. For more details, the antenna array arrangement in basic format can be imposed with the architecture of the neural networks like [10]:

- Input neurons of the neural network depends on the number of the array elements (antenna array) in as chosen by the user.
- Hidden neuron can influence in neural network weights and as well in antenna array structure, then updating (passing backwards weight adjustments) and correcting the weights until some satisfactory error level is reached.
- The desired response or the references signals that permit to obtain minimum errors correspondingly to the optimum solution through proper updating weight (convergence weight) to adapt the neural architecture and the phased array antenna configuration to result in both cases the optimizing state.

- Output neurons as the output signal from the array factor of antenna structure after optimization to form desired behavioral pattern with minimum of distortion and noiseless.

The Figure 5 presents a comparable diagramm between artificial neural network (ANN) architecture and phased array antenna structure in form multi-layer propagation network.

To check if the neural network can generate the required array pattern and their properties. The training of the artificial neural network (ANN) models for the synthesis is carried out using the

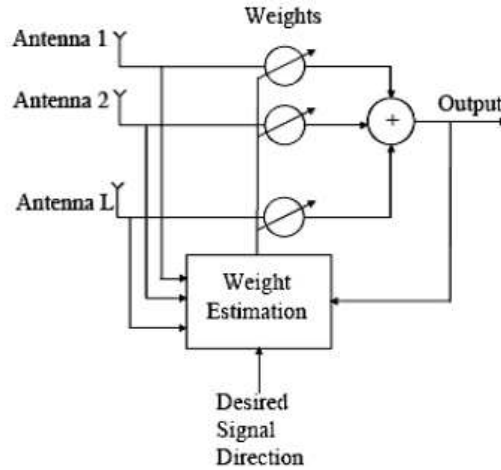


**Figure 5.** Block diagram of smart antenna array beamformer.

**Table 1.** Artificial neural network (ANN) training parameters.

Number of input neurons	1000
Number of hidden layers	2
Number of output neurons	1
Algorithm	<i>lm</i>
Learning rate	0.01
Momentum	0.95
MSE goal	$1e^{-1}$
Maximum validation failures	10
Minimum performance gradient	$1e^{-5}$
Initial mu	0.001
mu decrease factor	0.1
mu increase factor	10
Maximum mu	$1e^{10}$
Epochs between displays	25
Generate command-line output	false
Show training GUI	true
Maximum time to train in seconds	inf
Maximum number of epochs	300
Regularization parameter	0.8
Transfer function in hidden layer	tan-sigmoid (“tansig”)
Transfer function in output layer	linear(“purelin”)

Levenberg-Marquardt minimization method (the corresponding Matlab function is “trainlm”). The accuracy of the artificial neural network (ANN) models is evaluated by mean sum of squared error (MSE) between the calculated by analytic formula and the predicted values for the training data set.

Table 1 resumes the artificial neural network (ANN) training parameters and architectural parameters prepared for developing the artificial neural network (ANN) models.

#### 4. RESULTS AND OBSERVATION

##### 4.1. Analytic Results

To simulate circular antenna arrays configuration, it is necessary to consider an array antenna in uniform circular type that can also have an uniform spacing between elements. The considered elements are taken to be isotropic sources; so its radiation pattern can be described by its array factor. Starting from this known structure, we built respectively a concentric circular shaped extension of multiple ring antenna arrays with the same number of elements and different radii form a concentric circular array.

For the verification and the validation of simulation results, we proposed the patterns which are illustrated in Figure 6 and corresponding to both of cases: one ring array and uniformly excited and equally spaced concentric circular ring array.

The extension of uniform circular kind is more straight forward. Let’s assume we have a concentric circular antenna array (CCAA) (with multiple concentric circular rings) in the  $(x, y)$  plane, with positions given by:  $N_1 = N_2 = N_3 = N_4 = 12$  elements,  $N_0 = 1$  central element,  $R_1 = \lambda$ ,  $R_2 = 2\lambda$ ,  $R_3 = 3\lambda$ ,  $R_4 = 4\lambda$ . This array is plotted in Figure 7. Also, we simulate the array factor of the proposed concentric circular antenna grid. The result is presented in the same Figure 7.

For a better understanding of these results, we are proposed to study the resulting array factor response with another manner based on the Table 2. As illustrated in the same Table 2, this array configuration presents a better performance in terms Directivity, HPBW and SLL of the proposed structure were evaluated at various rings (with the same number of elements). The result shows that by increasing number of elements, higher values of directivity can be achieved. Similar trends can be observed in HPBW and SLL. We can notice the reduction in SLL with narrow beamwidth (half power beamwidth), but the paid cost is the increase in the aperture compared to uniform circular antenna grid (UCCA).

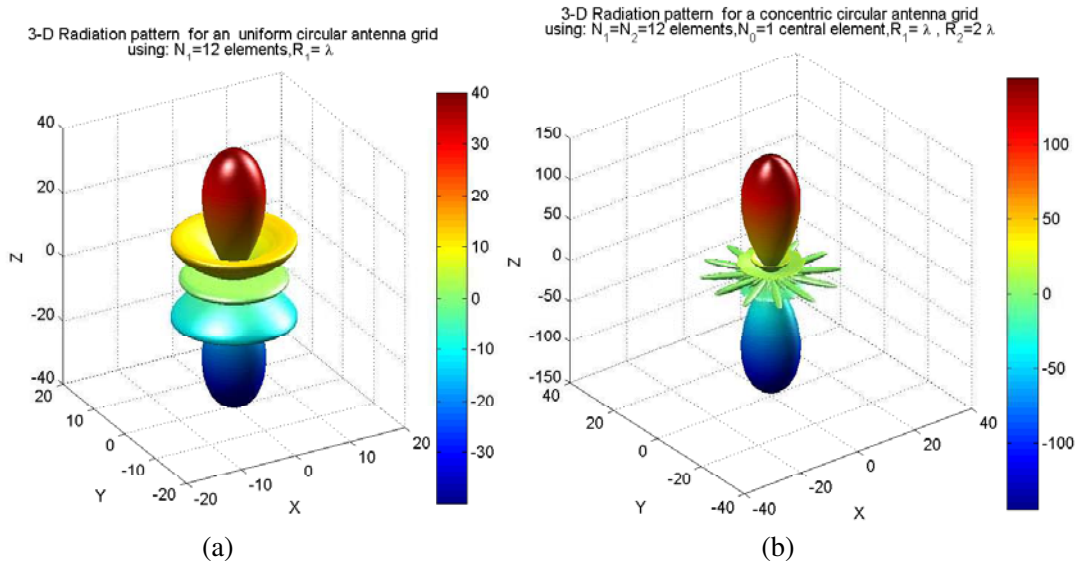


**Figure 6.** (a) (3-D) radiation pattern for an uniform circular antenna (UCA) grid using:  $N_1 = 12$  elements,  $R_1 = \lambda$ . (b) (3-D) radiation pattern for a concentric circular antenna (CCA) grid using:  $N_1 = N_2 = 12$  elements,  $N_0 = 1$  central element,  $R_1 = \lambda$ ,  $R_2 = 2\lambda$ .

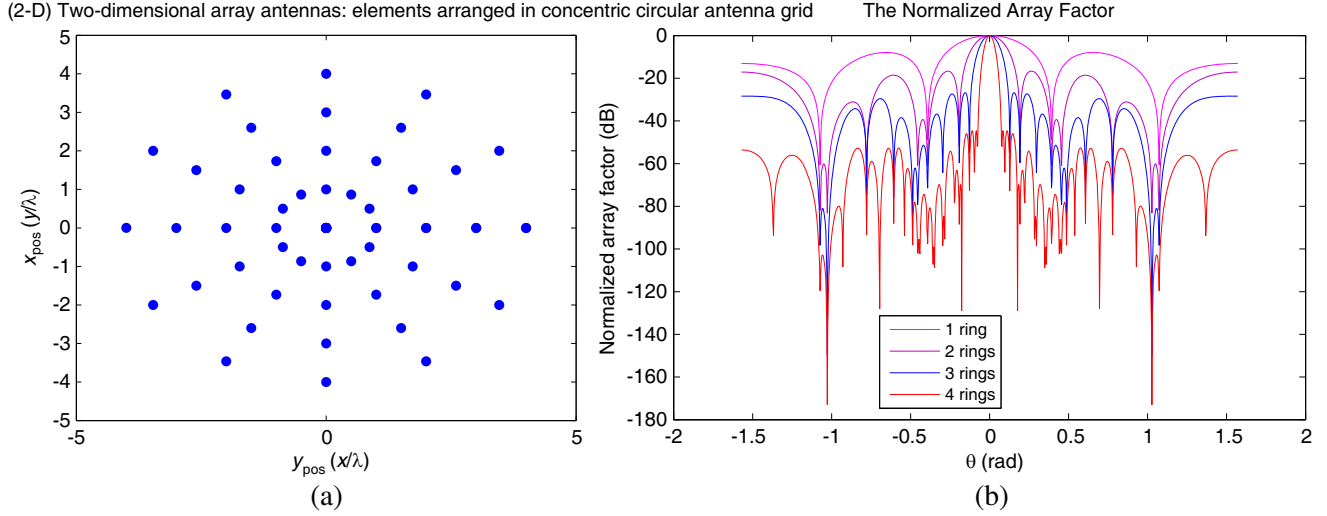


**Figure 7.** (a) (2-D) two-dimensional array antennas: elements arranged in concentric circular antenna grid. (b) The normalized array factor using:  $N_1 = N_2 = N_3 = N_4 = 12$  elements,  $N_0 = 1$  central element,  $R_1 = \lambda$ ,  $R_2 = 2\lambda$ ,  $R_3 = 3\lambda$ ,  $R_4 = 4\lambda$ .

**Table 2.** The performance parameters of the cases presented.

Rings	Directivity (dB)	SLL (dB)	HPWB ( $^\circ$ )	Gain-beamwidth product ( $^\circ$ )	Peak gain
1	38.1151	-7.9	28.1	337.49	12.0 (10.8 dBi)
2	46.7659	-16.7	12.7	1822.29	144.0 (21.6 dBi)
3	57.9632	-26.8	7.7	13360.65	1727.4 (32.4 dBi)
4	64.9851	-34.7	5.3	109273.69	20721.5 (43.2 dBi)

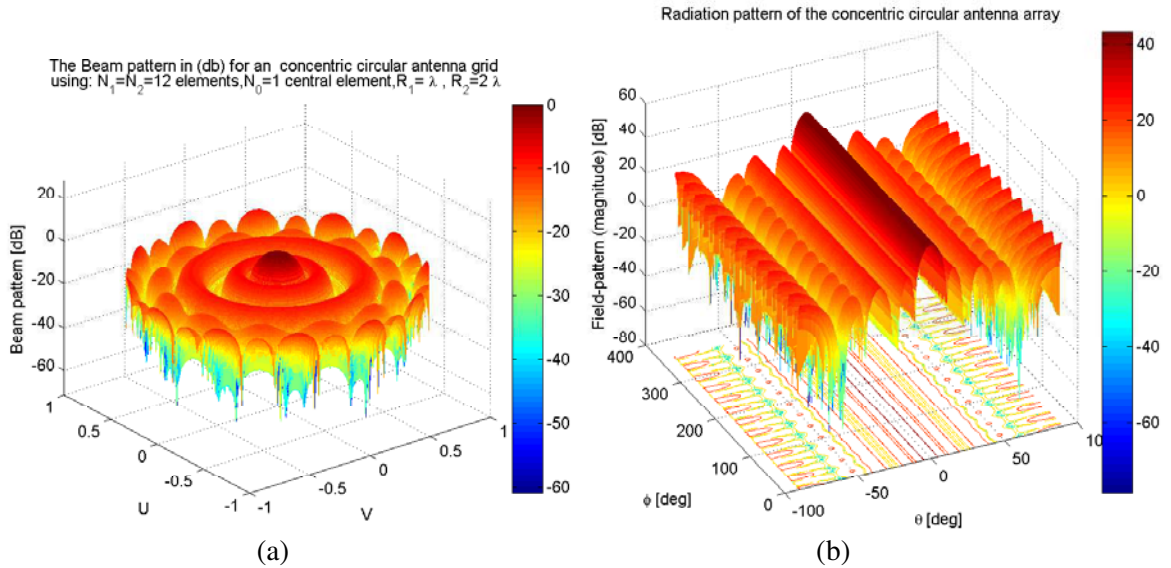


**Figure 8.** (a) The beam pattern in (dB) for a concentric circular antenna grid. (b) (3-D) results of the electric field as a function of the  $\theta$  and  $\phi$  directions using:  $N_1 = N_2 = 12$  elements,  $N_0 = 1$  central element,  $R_1 = \lambda$  and  $R_2 = 2\lambda$ .

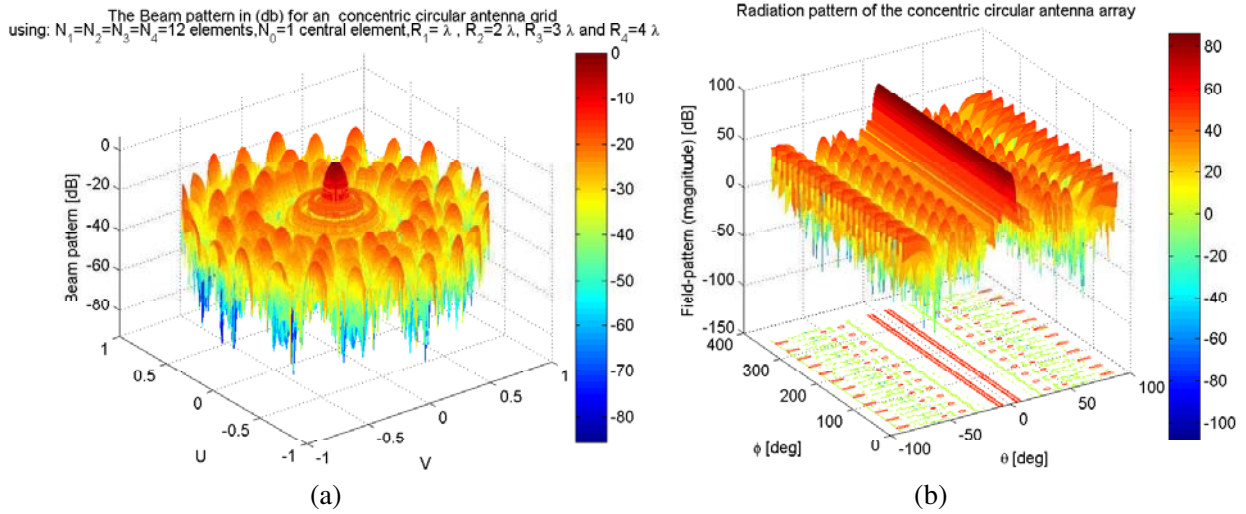


**Figure 9.** (a) The beam pattern in (dB) for a concentric circular antenna grid. (b) (3-D) results of the electric field as a function of the  $\theta$  and  $\phi$  directions using:  $N_1 = N_2 = N_3 = N_4 = 12$  elements,  $N_0 = 1$  central element,  $R_1 = \lambda$ ,  $R_2 = 2\lambda$ ,  $R_3 = 3\lambda$  and  $R_4 = 4\lambda$ .

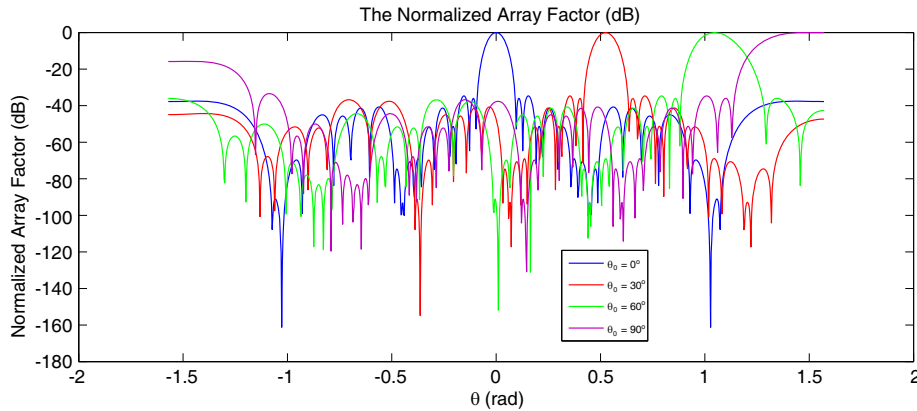


**Figure 10.** The array factor (AF) value in (dB) against  $\theta_0$  steering direction using:  $\phi_0 = 0^\circ$ ,  $N_1 = N_2 = N_3 = N_4 = 12$  elements,  $N_0 = 1$  central element,  $R_1 = \lambda$ ,  $R_2 = 2\lambda$ ,  $R_3 = 3\lambda$  and  $R_4 = 4\lambda$ .

To plot the array function expression, we will introduce simplifying variables,  $u = \frac{K_x \lambda}{2\pi} = \sin(\theta) \cos(\phi)$  and  $v = \frac{K_y \lambda}{2\pi} = \sin(\theta) \sin(\phi)$ . Also, the above variables are often used in plotting two-dimensional patterns, and are known as directional cosines (or  $(u, v)$  space). A plot of the AF above is shown in Figures 8 and 9: As expected, the array is maximum when  $(u, v) = (0, 0)$ , which corresponds to the desired direction ( $\theta = 0, \phi = 0$ ).

Figures 8 and 9 show a 3-D graph of the propagation of the electric field in the  $\theta$  and  $\phi$  directions, for all corresponding CCAA structures.

The same Figures 8 and 9 confirm that the main lobe of radiation pattern is reduced by increasing ring number. It is clear from Figure 10 that there is only one maximum that occurs at  $(\theta_0, \phi_0 = 0^\circ)$  while steering the main beam and does not have any grating lobe at  $\pi - \theta$ . Following the Figures 11 and 12, considering the  $(\theta_0, \phi_0 = 0^\circ)$  values, radiation properties of a concentric circular array of centrally fed radiators are analyzed that shows its better performance in terms of directivity, gain and also full 360° azimuth scanning. An advantage of this proposed phased array, compared to other type of array antenna

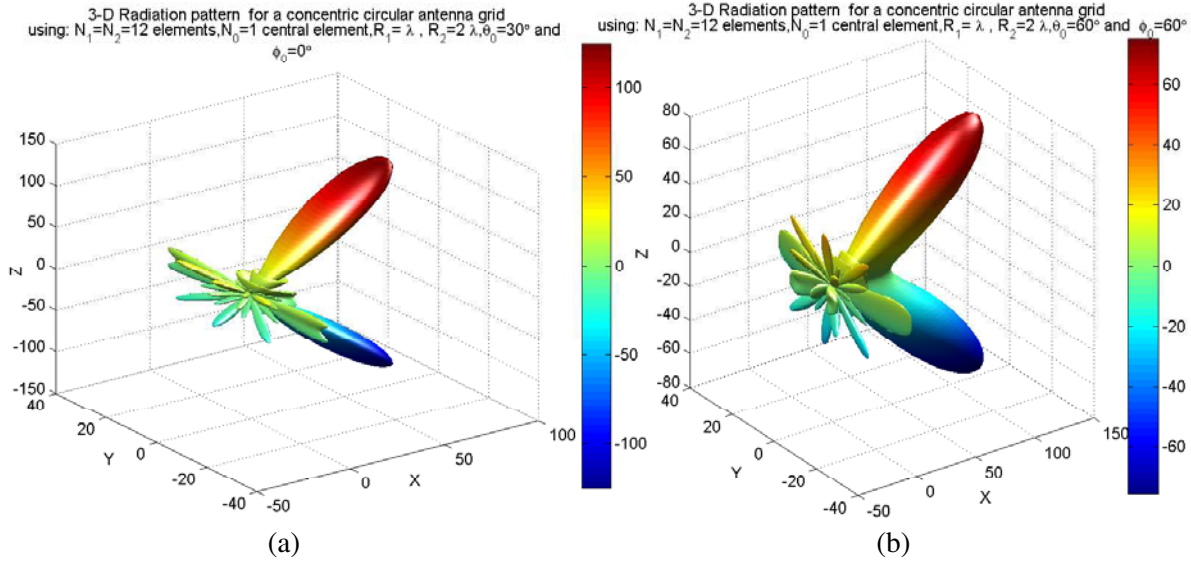


**Figure 11.** (3-D) radiation beam pattern steering of proposed array (concentric circular antenna grid). (a) ( $\phi_0 = 0^\circ, \theta_0 = 60^\circ$ ). (b) ( $\phi_0 = 60^\circ, \theta_0 = 60^\circ$ ) using:  $N_1 = N_2 = 12$  elements,  $N_0 = 1$  central element,  $R_1 = \lambda$  and  $R_2 = 2\lambda$ .

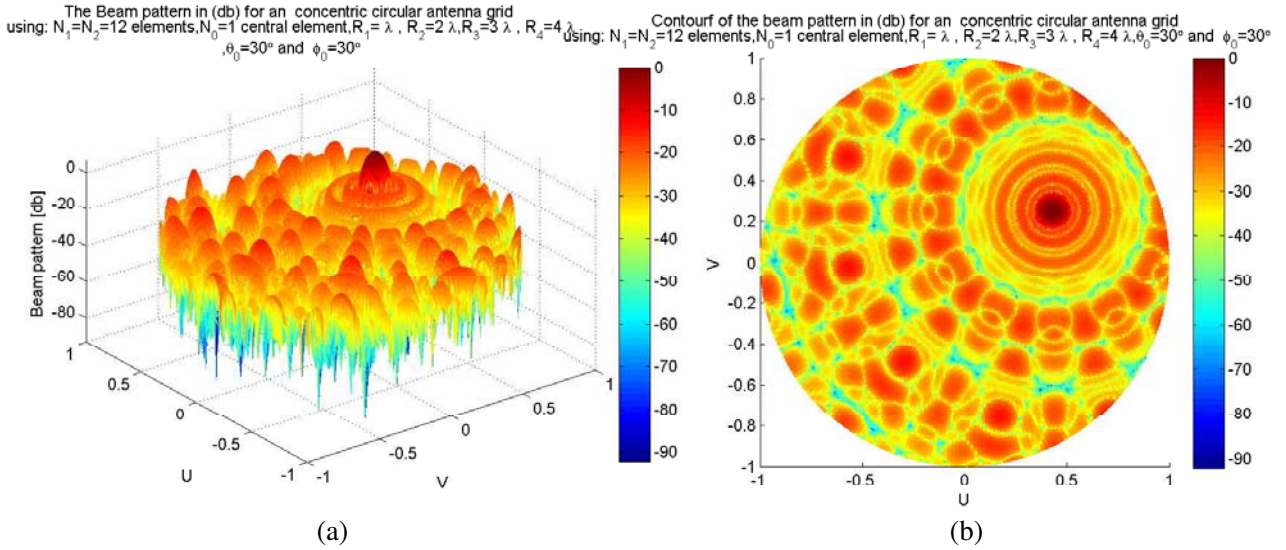


**Figure 12.** (a) The beam pattern in (dB) for a concentric circular antenna grid where ( $\phi_0 = 30^\circ, \theta_0 = 30^\circ$ ) using:  $N_1 = N_2 = N_3 = N_4 = 12$  elements,  $N_0 = 1$  central element,  $R_1 = \lambda$ ,  $R_2 = 2\lambda$ ,  $R_3 = 3\lambda$  and  $R_4 = 4\lambda$ .

configurations, is that the main beam can be electronically steered for a desired direction. The next example given in the Figure 12 illustrates the idea of phase steering. Similarly, the example scans the main beam of the array from +30 degrees azimuth, with elevation angle fixed at +30 degrees during the scan.

### 4.2. Artificial Neural Network (ANN) Application

In our application, the desired diagram is specified from a mask, the database contains a whole of data obtained by simulation with the previous study (analytic solution). In this work, we are interested to apply only planar array antennas arranged in a concentric circular grid. As mentioned before, the uniform circular array (one ring array) should certainly follow the same network procedure. After several tests, an artificial neural network (ANN) with the following geometry (see Figure 1) was retained: Two commonly used methods applied to overcome over-training problem, i.e., to decide when to stop training process, are early stopping (ES) and regularization methods. ES is widely used because it is easy to understand and implement also it has been reported to be superior to regularization methods. In order to use the ES method, the available normalized array factor's data must be divided into three sets, as presented in the Figure 13:

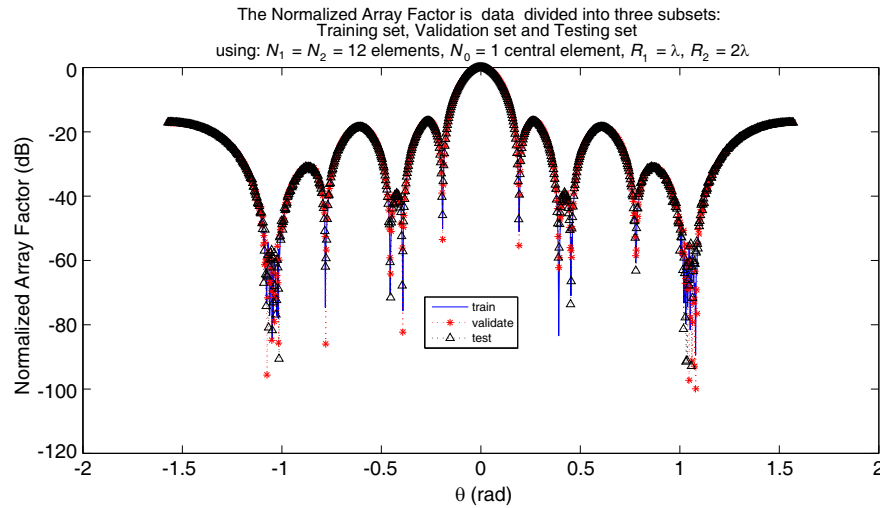


**Figure 13.** The normalized array factor is data divided into three subsets: Training set, Validation set and Testing set. The parameters which chosen to simulate the suggested three-dimensional array antennas are:  $\phi = 0$  rad,  $N_1 = N_2 = 12$  elements,  $N_0 = 1$  central element,  $R_1 = \lambda$  and  $R_2 = 2\lambda$ .

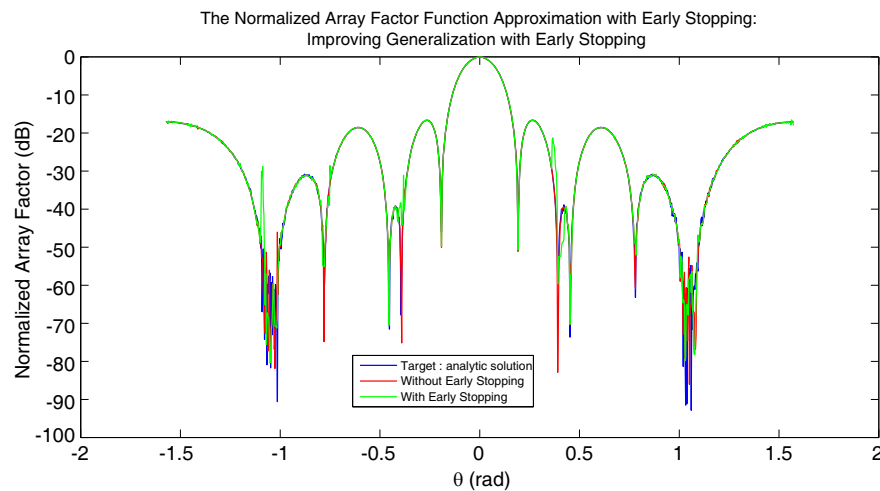


**Figure 14.** The normalized array factor function approximation with Early Stopping (ES): Improving Generalization with Early Stopping (ES). The parameters which chosen to simulate the suggested Three-dimensional array antennas are:  $\phi = 0$  rad,  $N_1 = N_2 = 12$  elements,  $N_0 = 1$  central element,  $R_1 = \lambda$  and  $R_2 = 2\lambda$ .

- Training set, used to determine artificial neural network (ANN) weights.
- Validation set, used to check the artificial neural network (ANN) performance and decide when to stop the training process.
- Test set, used to assess performance capabilities of developed artificial neural network (ANN) model.

A more detailed description of the ES method is graphically illustrated in the Figure 14. The methodology of ES method can be explained in [18].

From the Figure 14, we can see a good accuracy improvement generalization of the normalized array factor with Early Stopping (ES) technique. However, artificial neural network (ANN) based on ES method (Network with early stopping) is able to generate very fast the results of synthesis comparing to default artificial neural network (ANN) (Network without early stopping) which needs much more CPU time and memory. In consequence, Network with ES method can better fit the test data set with less discrepancies, therefore the early stopping feature can be used to prevent over-fitting of network towards the training data.

### 4.3. Artificial Neural Network (ANN) Performance

The computer code for training the artificial neural network (ANN) and measuring its performance was implemented under MATLAB environment. The network was executed with the set of knowledge base data of Normalized Array Factor. It shows the over all progress of the network. It clearly indicates that the training stops on reaching the maximum validation checks of 10. The number of epoch with 12 iterations and the performance (MSE) with 11.1, gradient decent value of 1.79 and mu value of 1.00.

Under training the curve, of the overall progress of the artificial neural network (ANN), indicates the 2 layer neural network training state plot for network with 1000 input nodes and 1 output nodes with combination structure as (1-2-1). The training stops when the validation parameter max\_fail reached maximum 10 validation checks at epoch 12 with the gradient decent value 1.7896 with reasonable Mu value 1.00 which would cause the convergence of the network fast. Because it could be expected that too small Mu value would cause the network to converge too slowly. As seen in Figure 15, the best validation performance is reached at epoch 2 and mean squared error (mse) for testing the data is 538.5015. In this example, the result is reasonable because of the following considerations:

- The final mean-square error is small.
- The test set error and the validation set error have similar characteristics.
- No significant over-fitting has occurred by iteration 3 (where the best validation performance occurs).

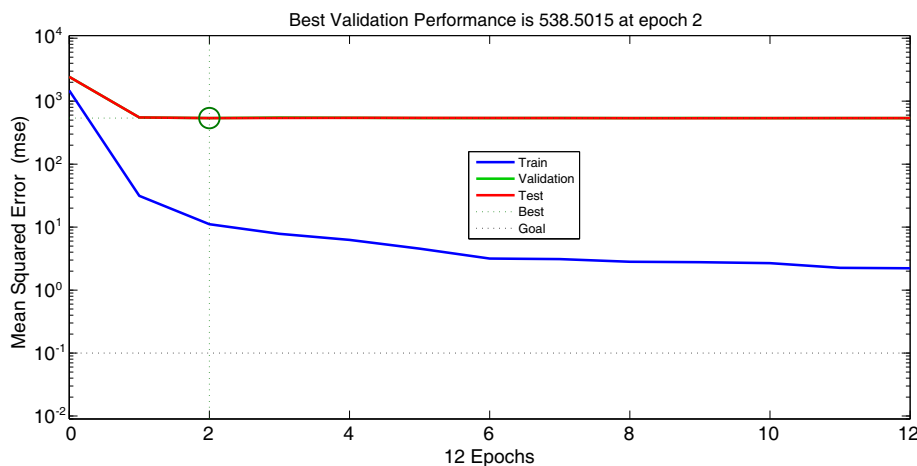


**Figure 15.** Evaluation of mean squared error.

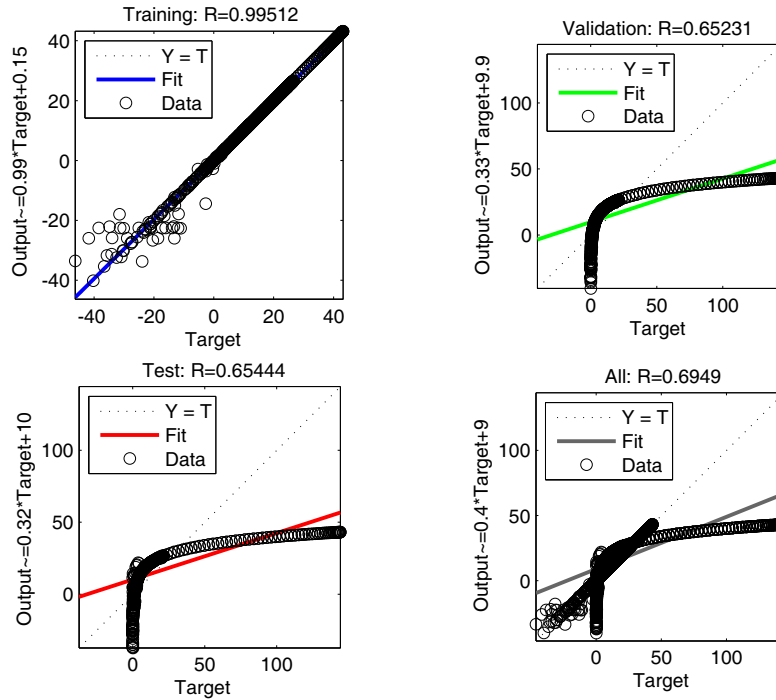


Figure 16. Regression plot of network.

Table 3. Time consumption learning presented on the overall progress of the artificial neural network (ANN).

Training	time consumed by the algorithm (second)
Default training (with levenberg algorithm)	3753.685
Training with early stopping method (using levenberg algorithm)	139.68

The regression analysis was obtained by artificial neural network (ANN) model after the network concludes training, testing and validation. In the training window, we can perform a linear regression between the network outputs and the corresponding targets. The following Figure 16 shows the results of the regression plot of training, test, validation and over all regression. The small circle shows the data representation in the model. After the regression plot has been evaluated, it's important to take under consideration and fitting the goodness of the diagnosis of the modelis. As all most approaches used coefficient of determination proof for goodness of fit includes  $R$  squared expressed as  $R^2$ , indicates how well the data points fit a line or curve. In the below figure the best fit was denoted as straightline. The dotted line presents the outputs equal to targets ( $Y = T$ ). The relationship between the outputs and the targets are provided by the Regression ( $R$ ) value for every network architecture. If  $R = 1$ , this proves the exact linear Relationship ( $R$ ) between outputs and targets. Practically, the  $R$  value would tend to obtain rarely a perfect value. From all these graphs, best regression value for validating the data is equal to  $R = 0.65231$ , regression value for testing the data is defined as  $R = 0.65444$ , regression value for training the data is defined as  $R = 0.99512$  and overall regression value is  $R = 0.6949$ . This proves the developed model and the network procedure of training, testing and validation are significantly valid [12, 13].

To show the speed of the computation time, the difference consumption time between default training and training with early stopping method (using levenberg algorithm) is given in the Table 3. It proves that the elapsed time of an early stopping method is less important than the time needed for a default training (without early stopping).

## 5. CONCLUSION

This article presents the limitation of uniform circular antenna arrays to increase the gain and the directivity pattern. To enhance the radiation characteristics, we propose to grow up the array elements numbers by introducing a concentric circular antenna configuration. Based on this simple geometry, it's possible to study other aperiodic (random cases) arrays of various three dimensional (3D) geometries (e.g., conformal phased array antenna). This analyze is necessary starting point for future investigation of neural network solution for irregular antenna array synthesis. The adoption of the early stopping method permits to use neural network with reduced complexity. Network contains as little neurons as possible. If we are lucky, it will be so flexible that it will be able to train — It is more flexible to overfit. Due to the early stopping technique, the neural network training results in a very important gain in the running time and the used memory.

For a future work, we suggest to apply the optimisation techniques (genetic, LMS,.. etc.) in concentric circular antenna arrays to predict the desired radiation that can be adopted to increase the gain and to scan the range by suppressing sidelobe level (SLL).

## REFERENCES

1. Luo, Z., X. He, X. Chen, X. Luo, and X. Li, "Synthesis of thinned concentric circular antenna arrays using modified TLBO algorithm," *International Journal of Antennas and Propagation*, Vol. 2015, 9 pages, Article ID 586345, 2015.
2. Albagory, Y. and O. Said, "Optimizing concentric circular antenna arrays for high-altitude platforms wireless sensor networks," *I.J. Computer Network and Information Security*, Vol. 5, 1–8, 2014.
3. Reyna Maldonado, A., M. A. Panduro, and C. del Rio-Bocio, "On the design of concentric ring array for isoflux radiation in Meo satellites based on PSO," *Progress In Electromagnetics Research M*, Vol. 20, 243–255, 2011.
4. Reynaa, A., M. A. Panduroa, D. H. Covarrubias, and A. Mendez, "Design of steerable concentric rings array for low side lobe level," *Scientia Iranica*, Vol. 19, No. 3, 727–732, Jun. 2012.
5. Zhang, L., Y.-C. Jiao, and B. Chen, "Optimization of concentric ring array geometry for 3D beam scanning," *International Journal of Antennas and Propagation*, Vol. 2012, 5 pages, Article ID 625437, 2012.
6. Yan, K.-K. and Y. Lu, "Sidelobe reduction in array-pattern synthesis using genetic algorithm," *IEEE Transactions on Antennas and Propagation*, Vol. 45, No. 7, Jul. 1997.
7. Mandal, D., S. P. Ghoshal, and A. K. Bhattacharjee, "Optimized radii and excitations with concentric circular antenna array for maximum sidelobe level reduction using wavelet mutation based particle swarm optimization techniques," *Telecommunication Systems*, Vol. 52, No. 4, 2015–2025, Apr. 2013.
8. Elsaidy, E. I., M. I. Dessouky, S. Khamis, and Y. A. Albagory, "Concentric circular antenna array synthesis using comprehensive learning particle swarm optimizer," *Progress In Electromagnetics Research Letters*, Vol. 29, 1–13, 2012.
9. Rawata, A., R. N. Yadavb, and S. C. Shrivastavac, "Neural network applications in smart antenna arrays: A review," *AEU — International Journal of Electronics and Communications*, Vol. 66, No. 11, 903–912, Nov. 2012.
10. Zaharis, Z. D., K. A. Gotsis, and J. N. Sahalos, "Comparative study of neural network training applied to adaptive beamforming of antenna arrays," *Progress In Electromagnetics Research*, Vol. 126, 269–283, 2012.
11. Guo, H., C.-J. Guo, Y. Qu, and J. Ding, "Pattern synthesis of concentric circular antenna array by nonlinear least-square method," *Progress In Electromagnetics Research B*, Vol. 50, 331–346, 2013.
12. Dudeczyk, J. and A. Kawalec, "Adaptive forming of the beam pattern of microstrip antenna with the use of an artificial neural network," *International Journal of Antennas and Propagation*, Vol. 2012, 13 pages, Article ID 935073, 2012.

13. Ali, B. A. A., M. S. Salit, E. S. Zainudin, and M. Othman, "Integration of artificial neural network and expert system for material classification of natural fibre reinforced polymer composites," *American Journal of Applied Sciences*, Vol. 12, No. 3, 174–184, Apr. 2015.
14. Ghayoula, R., N. Fadlallah, A. Gharsallah, and M. Rammal, "Phase-only adaptive nulling with neural networks for antenna array synthesis," *IET Microw. Antennas Propag.*, Vol. 3, No. 1, 154–163, 2009.
15. Merad, L., F. T. Bendimerad, S. M. Meriah, and S. A. Djennas, "Neural networks for synthesis and optimization of antenna arrays," *Radioengineering*, Vol. 16, No. 1, Apr. 2007.
16. Kapetanakis, T. N., I. O. Vardiambasis, G. S. Lioudakis, M. P. Ioannidou, and A. M. Maras, "Smart antenna design using neural networks," *8th International Conference: New Horizons in Industry, Business and Education (NHIBE 2013)*, 130–135, Chania, Greece, 2013.
17. Pei, B., H. Han, Y. Sheng, and B. Qiu, "Research on smart antenna beamforming by generalized regression neural network," *2013 IEEE International Conference on Signal Processing, Communication and Computing (ICSPCC)*, 2013.
18. Wang, L., H. C. Quek, K. H. Tee, N. Zhou, and C. Wan, "Optimal size of a feedforward neural network: How much does it matter?," *Joint International Conference on Autonomic and Autonomous Systems and International Conference on Networking and Services*, Papeete, Tahiti, Oct. 23–28, 2005.